ISSN 0020-1685, Inorganic Materials, 2018, Vol. 54, No. 1, pp. 8–16. © Pleiades Publishing, Ltd., 2018.
Original Russian Text © L.F. Mashadieva, Z.T. Gasanova, Yu.A. Yusibov, M.B. Babanly, 2018, published in Neorganicheskie Materialy, 2018, Vol. 54, No. 1, pp. 11–18.

Phase Equilibria in the $Cu_2Se–Cu_3AsSe_4–Se$ System and Thermodynamic Properties of Cu_3AsSe_4

L. F. Mashadieva[a], Z. T. Gasanova[b], Yu. A. Yusibov[c], and M. B. Babanly[a, *]

[a] *Nagiyev Institute of Catalysis and Inorganic Chemistry, Academy of Sciences of Azerbaijan, H. Javid ave. 113, Baku, AZ 1143 Azerbaijan*

[b] *Baku State University, Z. Khalilov str. 23, Baku, AZ 1143 Azerbaijan*

[c] *Ganja State University, pr. G. Alieva 187, Ganja, AZ 2000 Azerbaijan*

**e-mail: babanlymb@gmail.com*

Received July 4, 2016; in final form, May 30, 2017

Abstract—The $Cu_2Se–Cu_3AsSe_4–Se$ system has been studied using differential thermal analysis, X-ray diffraction, and emf measurements on concentration cells using $Cu_4RbCl_3I_2$ as a solid electrolyte. We have constructed a number of vertical sections through the phase diagram, the room-temperature solid-state phase compatibility diagram, and a projection of the liquidus surface. The primary crystallization fields of the phases present and the types and coordinates of in- and univariant equilibria in the system have been identified. The system has been shown to contain a broad liquid–liquid immiscibility region. Using emf data, we evaluated the standard thermodynamic functions of formation and standard entropy of the Cu_3AsSe_4 compound.

Keywords: Cu–As–Se system, phase diagram, liquidus surface, copper arsenic selenides, Cu_3AsSe_4 compound, thermodynamic properties

DOI: 10.1134/S0020168518010090

INTRODUCTION

Ternary copper chalcogenides are promising functional materials for advanced engineering applications. Many of them possess attractive thermoelectric, photoelectric, optical, and other properties [1–6] and some of them are superionic conductors with high Cu^+ ion conductivity and are thought to have considerable potential for use as ion-selective electrodes, solid electrolytes, etc. [7, 8].

The Cu–As–Se system has attracted increased interest because both crystalline and glassy phases in this system possess functional properties of practical importance [9, 10].

Data on the phase equilibria in the Cu–As–Se system and the properties of its ternary phases reported before the early 1990s were summarized in a number of publications [2, 3, 11]. In a somewhat later report, Cohen et al. [12] presented new data on phase equilibria in this system, which differed from what had been reported previously. In particular, from the ternary compounds Cu_3AsSe_4, $CuAsSe_2$, Cu_3AsSe_3, and $Cu_6As_4Se_9$ described in the literature, only the first two were represented in the phase diagram mapped out by Cohen et al. [12]. Unfortunately, Cohen et al. [12] presented no references to previous research and, accordingly, no comparative analysis of their results and previously reported data. Comparison of available data suggests that, even though a number of vertical sections in the Cu–As–Se system have been studied, there is still no reliable picture of phase equilibria in the Cu–As–Se system.

Given the above, we undertook a new, detailed study of phase equilibria in the Cu–As–Se system. In this paper, we present our results on phase equilibria in the $Cu_2Se–Cu_3AsSe_4–Se$ subsystem and the thermodynamic properties of the Cu_3AsSe_4 compound.

The phase diagrams of the constituent binary system Cu–Se in modern handbooks [1, 13, 14] are almost identical. According to available data, this system contains the following compounds: Cu_2Se, Cu_3Se_2, CuSe, and $CuSe_2$. The first compound melts congruently at 1403 K. The second compound exists below 385 K. At this temperature, it decomposes by a solid-state reaction. The other two compounds decompose peritectically at 650 and 605 K, respectively. The Cu_2Se compound undergoes a polymorphic transformation at 396 K (at 435 K according to Abrikosov [1]), and CuSe undergoes polymorphic transformations at 393 and 324 K. The homogeneity range of Cu_2Se is located at selenium-enriched compositions and has the largest extent at 800 K: from 33.3 to 36.6 at % Se [13].

The liquidus of the Cu_2Se–Se subsystem consists of only the primary crystallization curve of the high-temperature phase of Cu_2Se. The liquidus curves of CuSe, $CuSe_2$, and elemental selenium are degenerate. The system contains a broad liquid–liquid immiscibility region, which extends from 52.5 to ~99 at % Se at the monotectic equilibrium temperature (796 K).

Published data on the melting behavior and melting point of Cu_3AsSe_4 are contradictory. According to Blachnik and Gather [15], this compound melts incongruently at 733 K, whereas according to Abrikosov [1] and Potorii [16] it melts congruently at 750 K and undergoes a polymorphic transformation at 715 K. Its low-temperature phase has a tetragonal structure, and its high-temperature phase has a cubic structure.

Crystallographic parameters of the copper selenides and Cu_3AsSe_4 have been presented in a number of reports [1–3, 11–14].

EXPERIMENTAL

To synthesize the Cu_2Se, CuSe, $CuSe_2$, and Cu_3AsSe_4 compounds for assessing phase equilibria in the Cu_2Se–Cu_3AsSe_4–Se system, appropriate amounts of high-purity elemental components were melted together in silica ampules sealed off under a vacuum of ~10^{-2} Pa.

Cu_2Se was synthesized in an inclined two-zone furnace. The temperature of the lower, "hot" zone was 1420 K, and that of the upper, "cold" zone was 900 K, that is, slightly below the boiling point of selenium (958 K [17]). To obtain homogeneous, stoichiometric Cu_2Se, we followed recommendations by Glazov et al. [18]: after synthesis, the material was quenched from a temperature of 1300 K in cold water.

Given that the CuSe and $CuSe_2$ compounds melt incongruently, after their components were melted together at ~900 K the ampules were slowly cooled to temperatures of 620 and 580 K, respectively, where the samples were annealed for 500 h.

Cu_3AsSe_4 was synthesized at 900 K and then annealed at 700 K for 50 h.

All of the synthesized compounds were identified by differential thermal analysis (DTA) and X-ray diffraction.

To prepare alloys of the Cu_2Se–Cu_3AsSe_4–Se system, the constituent binary compounds, Cu_3AsSe_4, and elemental selenium were melted together in silica ampules sealed off under vacuum. From the DTA data for selected compositions of cast unhomogenized alloys, we determined suitable annealing temperatures (~30–50 K below the solidus), at which the alloys were held for 600–800 h. Experimental data indicated that, under such annealing conditions, the materials close in composition to the CuSe and $CuSe_2$ compounds did not reach equilibrium. Because of this, these materials were thoroughly ground into powder, properly mixed, pressed into disks, and annealed for an additional 300 h.

The alloys were characterized by DTA (Netzsch 404 F1 Pegasus system), X-ray diffraction (Bruker D8 Advance powder diffractometer), and emf measurements using concentration cells of the type

$$(-)\mathrm{Cu(s)}\left|\mathrm{Cu_4RbCl_3I_2(s)}\right|\mathrm{(Cu{-}As{-}Se)(s)}(+). \quad (1)$$

EMF measurements with $Cu_4RbCl_3I_2$ as a solid electrolyte were successfully used earlier in thermodynamic studies of some copper-containing ternary chalcogenides [8, 19–24].

The compound $Cu_4RbCl_3I_2$, used as a solid electrolyte in cells of the type (1), was prepared by melting stoichiometric ratios of reagent-grade anhydrous CuCl, CuI, and RbCl at 900 K in a silica ampule pumped down to ~10^{-2} Pa, followed by cooling to 450 K and homogenization by annealing at this temperature for 100 h [8]. The resultant cylindrical ingot ~8 mm in diameter was sliced into disks 4–6 mm thick, which were used as the solid electrolyte in cells of the type (1).

In the cells of the type (1), the right-hand electrodes were made from equilibrium alloys of the system under investigation and a few Cu_3AsSe_4 samples containing small (1–3 at %) As and Se excesses. The right-hand electrodes were produced by pressing powdered annealed alloys into disks ~8–10 mm in diameter and 4–6 mm in thickness. The procedures used to set up electrochemical cells and measure their emf were described in detail elsewhere [13, 14].

RESULTS AND DISCUSSION

A joint analysis of the present experimental data and published reports on the constituent pseudobinary system Cu_2Se–Se [13, 14] allowed us to obtain a self-consistent picture of phase equilibria in the Cu_2Se–Cu_3AsSe_4–Se subsystem. For convenience of comparison with the total T–x–y phase diagram of the Cu–As–Se system, the compositions in the subsystem under consideration are represented in the form Cu_2Se–$\frac{3}{8}Cu_3AsSe_4$–3Se, which is equivalent to expressing compositions as an atomic percent.

Constituent pseudobinary systems. The Cu_2Se–$\frac{3}{8}Cu_3AsSe_4$ system (Fig. 1a) has a eutectic T–x phase diagram. The eutectic composition is 10 mol % Cu_2Se, with a melting point at 743 K. Cu_3AsSe_4 has the highest solubility in the high-temperature phase of Cu_2Se at the eutectic temperature: ~6 mol %. The 715- and 400-K horizontals correspond to the polymorphic transformations of Cu_3AsSe_4 and Cu_2Se, respectively. The temperatures of these transitions coincide with those for the stoichiometric compositions of both

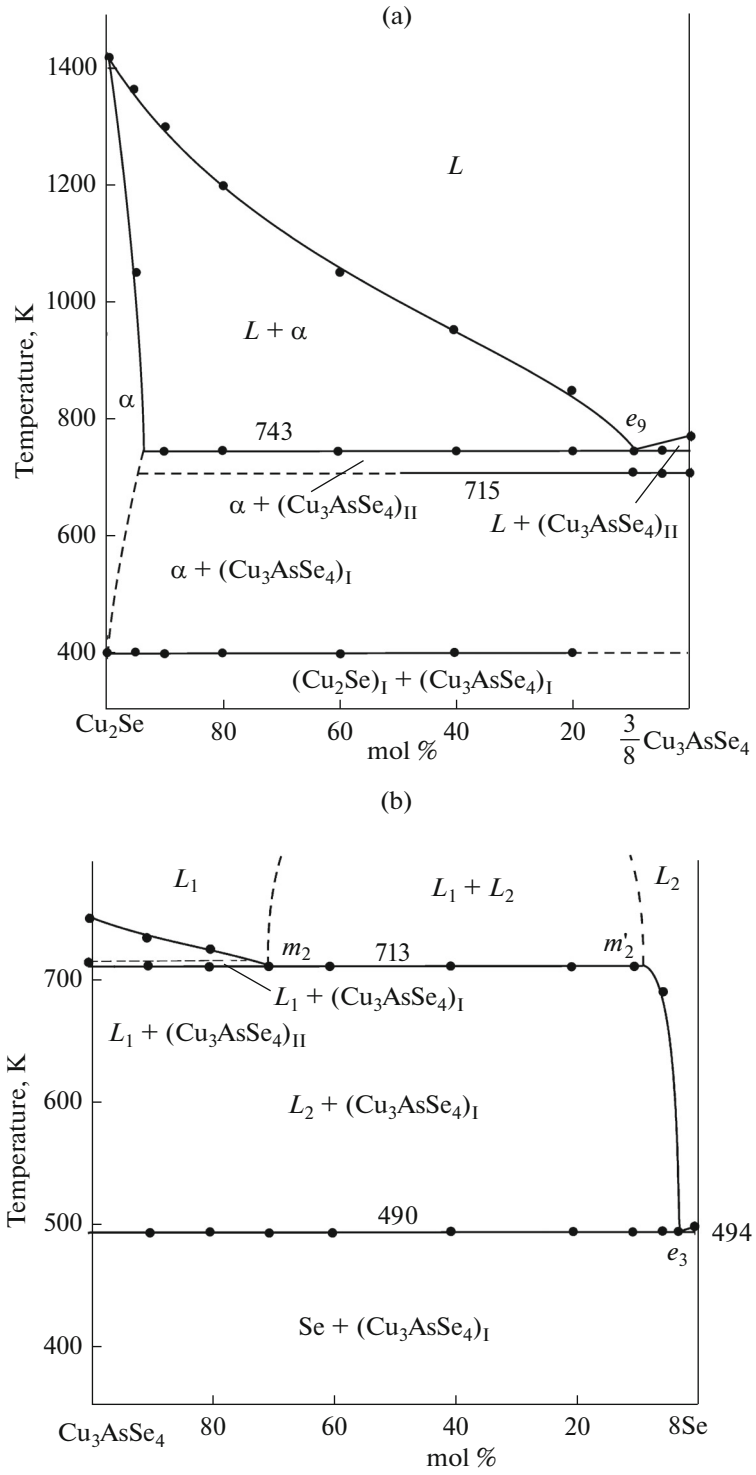

Fig. 1. Phase diagrams of the (a) Cu_2Se–Cu_3AsSe_4 and (b) Cu_3AsSe_4–Se systems.

compounds, suggesting that their mutual solubility near their transition temperatures is insignificant.

The Cu_3AsSe_4–8Se system (Fig. 1b) is characterized by monotectic (m_2m_2') and eutectic (e_3) equilibria. At the monotectic temperature (713 K), the liquid–liquid immiscibility region extends from ~8 to 70 mol % Cu_3AsSe_4. The eutectic composition is ~3 mol % Cu_3AsSe_4, with a melting point at 490 K. Any thermal events due to the phase transition of Cu_3AsSe_4 (715 K) were not detected experimentally because of the proximity to the monotectic temperature, so in Fig. 1b the phase transition is represented by a dashed line.

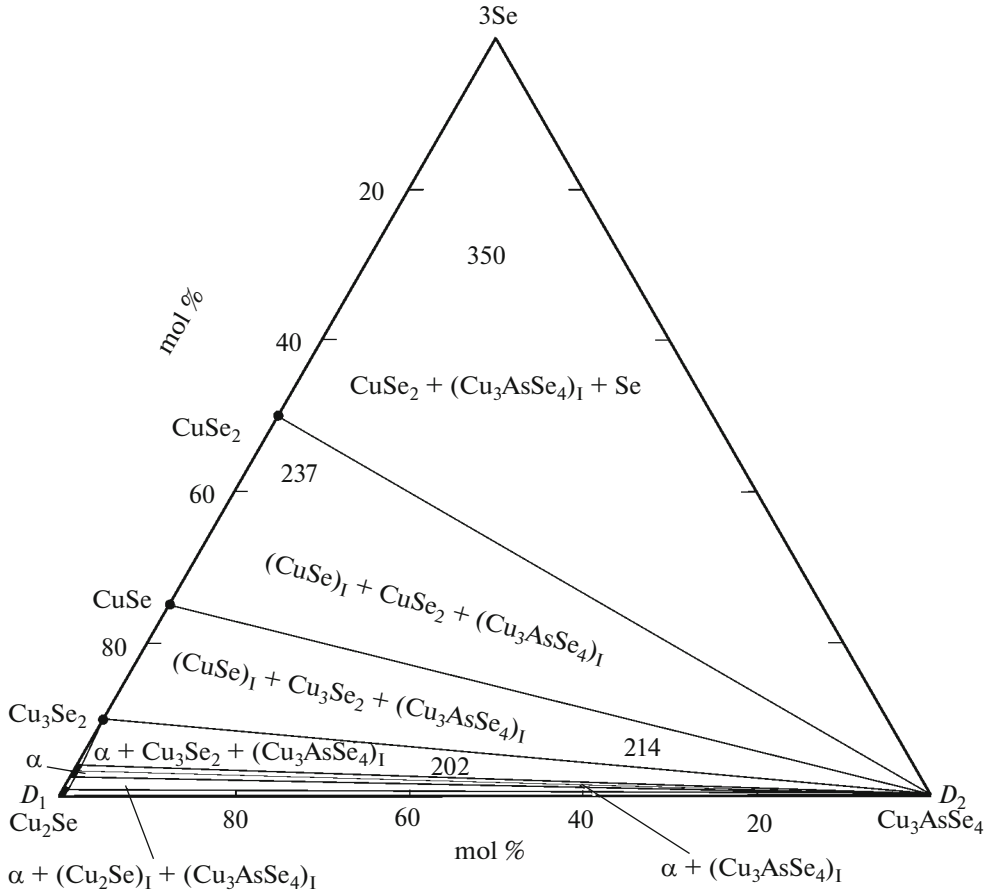

Fig. 2. Room-temperature phase relations in the Cu_2Se–Cu_3AsSe_4–Se system. The numbers in the three-phase fields specify the emf (mV) of concentration cells of the type (1).

Room-temperature phase relations. Figure 2 shows the room-temperature phase compatibility diagram of the Cu_2Se–Cu_3AsSe_4–Se system. It is seen that all of the copper selenides and the α-phase (based on the high-temperature Cu_2Se polymorph) have tie lines with Cu_3AsSe_4 and divide the composition triangle into five three-phase fields. The phase compositions of the alloys were determined by X-ray diffraction and confirmed by emf measurements with concentration cells of the type (1). It was found that, at a given temperature, the emf was constant within each three-phase field and changed sharply in going from one three-phase field to another (Fig. 2). The emf values obtained are similar to those reported previously in the literature [25], suggesting that, in the system under consideration, Cu_3AsSe_4 solubility in the copper selenides is insignificant.

Liquidus surface. The liquidus surface of the Cu_2Se–Cu_3AsSe_4–Se system (Fig. 3) comprises two major fields, corresponding to the primary crystallization of the (Cu_2Se-based) α-phase and Cu_3AsSe_4. On the liquidus surface of Cu_3AsSe_4, the primary crystallization fields of particular polymorphs of this compound are not separated. The primary crystallization fields of the CuSe and $CuSe_2$ compounds and elemental selenium are degenerate. This part of the T–x–y phase diagram is presented in Fig. 3 on an expanded scale (arbitrary scale).

A characteristic feature of the system under consideration is the broad liquid–liquid immiscibility region ($L_1 + L_2$), which has the form of a continuous strip between the monotectic horizontals of the Cu_2Se–Se (m_1m_1') and Cu_3AsSe_4–Se (m_2m_2') constituent binary systems. Crossing the immiscibility region, the eutectic curve issuing from point e_1 transforms into an invariant monotectic equilibrium (MM' horizontal). At the selenium corner of the composition triangle, a number of in- and univariant equilibria are degenerate. The types and temperatures of all the in- and univariant equilibria in the system are summarized in Tables 1 and 2.

Vertical sections. Below, we describe a number of vertical sections through the T–x–y phase diagram, which more clearly illustrate crystallization processes and solid-state transformations in the system. Con-

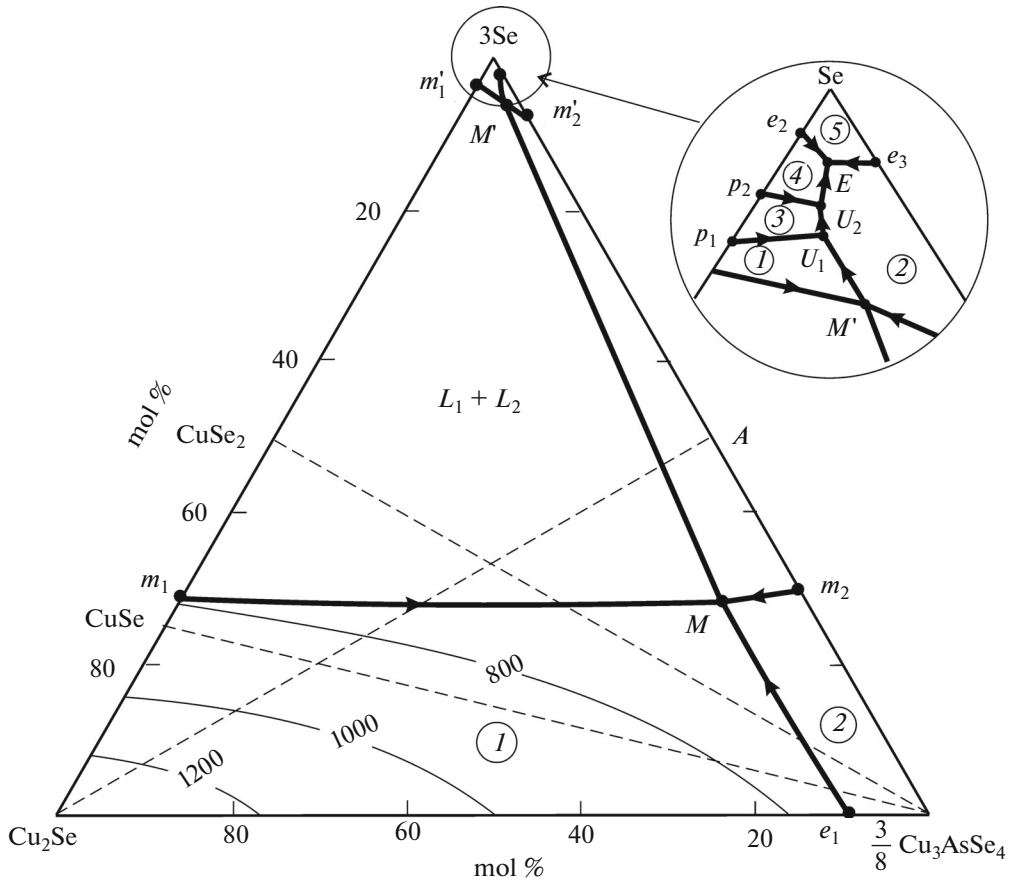

Fig. 3. Projection of the liquidus surface in the Cu_2Se–Cu_3AsSe_4–Se system. Primary crystallization fields: (*1*) α, (*2*) Cu_3AsSe_4, (*3*) $(CuSe)_{III}$, (*4*) $CuSe_2$, (*5*) Se. The dashed lines represent the vertical sections studied.

sider them in the context of Figs. 2 and 3 and Tables 1 and 2.

$4CuSe$–Cu_3AsSe_4 section (Fig. 4a). The liquidus consists of two curves, corresponding to the primary crystallization of the α-phase and the high-temperature phase of Cu_3AsSe_4. Below the liquidus, crystallization follows first the univariant monotectic reactions m_1M and e_1M and then the invariant monotectic reaction M, and ends with the invariant transition reaction U_1 (Fig. 3; Tables 1, 2). The last reaction yields a $(CuSe)_{III}$ + $(Cu_3AsSe_4)_I$ two-phase mixture. The 393- and 325-K horizontals correspond to the polymorphic transformations of CuSe, and the 715-K horizontal, to the polymorphic transformation of Cu_3AsSe_4.

$CuSe2$–Cu_3AsSe_4 section (Fig. 4b). The liquidus consists of two curves, corresponding to the α-phase and $(Cu_3AsSe_4)_I$. A part of the former curve lies in the liquid–liquid immiscibility region and reflects crystallization by the monotectic reaction $L_1 \leftrightarrow L_2 + \alpha$ (m_1M). The 695- and 645-K horizontals (U_1) correspond to the invariant monotectic (M) and transition (U_1) equilibria. Crystallization ends with the invariant transition reaction U_2 (605 K), so that the T–x phase diagram has a $CuSe_2$ + Cu_3AsSe_4 two-phase field (Figs. 2, 3; Table 1).

Cu_2Se–[A] section (Fig. 5). This section is of interest because it crosses all of the phase fields below the solidus (Fig. 2) and reflects essentially all of the in- and univariant equilibria in the Cu_2Se–Cu_3AsSe_4–Se system. The α-phase has a broad primary crystallization field, where it crystallizes from an L_1 melt (~45–100 mol % Cu_2Se) or from two immiscible liquid phases, $L_1 + L_2$ (~7–45 mol % Cu_2Se). $(Cu_3AsSe_4)_I$ has a narrow primary crystallization field (0–7 mol % Cu_2Se), where it crystallizes by the monotectic reaction m_2M. Crystallization continues by the invariant monotectic (M) and transition (U_1) reactions. In the composition range ~60–95 mol % Cu_2Se, crystallization ends with reaction U_1, leading to the formation of an α + $(CuSe)_{III}$ + $(Cu_3AsSe_4)_I$ three-phase field. At lower Cu_2Se concentrations, crystallization ends with a transition U_2 (34–59 mol % Cu_2Se) or eutectic E (0–34 mol % Cu_2Se) equilibrium process, which yields a $(CuSe)_{III}$ + $CuSe_2$ + $(Cu_3AsSe_4)_I$ or $CuSe_2$ + $(Cu_3AsSe_4)_I$ + Se three-phase mixture, respectively.

Table 1. Invariant equilibria in the Cu_2Se–Cu_3AsSe_4–Se system

Point in Fig. 3	Equilibrium	T, K
D_1	$L \leftrightarrow (Cu_2Se)_{II}$	1403
D_2	$L \leftrightarrow (Cu_3AsSe_4)_{II}$	750
$m_1(m_1')$	$L_1 \leftrightarrow L_2 + \alpha$	795
$m_2(m_2')$	$L_1 \leftrightarrow L_2 + (Cu_3AsSe_4)_I$	713
$M(M')$	$L_1 \leftrightarrow L_2 + \alpha + (Cu_3AsSe_4)_I$	695
p_1	$L + \alpha \leftrightarrow (CuSe)_{III}$	650
p_2	$L + (CuSe)_{III} \leftrightarrow CuSe_2$	605
U_1	$L + \alpha \leftrightarrow (CuSe)_{III} + (Cu_3AsSe_4)_I$	645
U_2	$L + (CuSe)_{III} \leftrightarrow CuSe_2 + (Cu_3AsSe_4)_I$	600
e_1	$L \leftrightarrow \alpha + (Cu_3AsSe_4)_{II}$	743
e_2	$L \leftrightarrow CuSe_2 + Se$	494
e_3	$L \leftrightarrow (Cu_3AsSe_4)_I + Se$	492
E	$L \leftrightarrow CuSe_2 + (Cu_3AsSe_4)_I + Se$	490

Here and in Table 2, α refers to the solid solutions based on the high-temperature phase of Cu_2Se, the low-temperature phases are labeled by the subscript I, and the high-temperature phases are labeled by the subscripts II and III.

The 393- and 325-K thermal events are the polymorphic transformations of CuSe, and the 385-K thermal event is the solid-state reaction $\alpha + (CuSe)_{II} = Cu_3Se_2$. This reaction leads to the formation of $\alpha + Cu_3Se_2 + (Cu_3AsSe_4)_I$ and $Cu_3Se_2 + (CuSe)_{II} + (Cu_3AsSe_4)_I$ three-phase fields (Fig. 2).

Thermodynamic properties of Cu_3AsSe_4. The emf measurements on cells of the type (1) for the Cu_3AsSe_4 samples containing 1–3 at % excess As and Se were used to evaluate the thermodynamic functions of the low-temperature phase of Cu_3AsSe_4. To this end, the emf data were analyzed using least squares fitting. We obtained the linear equation

$$E, \text{ mV} = 402.8 + 0.036T \pm 2\left[\frac{0.4}{26} + 3.4\times10^{-5}(T - 360.7)^2\right]^{1/2}, \quad (2)$$

represented in the form recommended by Morachevskii et al. [19].

Using Eq. (2) and well-known thermodynamic relations [19], we evaluated relative partial thermodynamic functions of the copper in Cu_3AsSe_4:

$$\Delta\bar{G}_{Cu} = -39.90 \pm 0.08 \text{ kJ/mol},$$

$$\Delta\bar{H}_{Cu} = -38.86 \pm 0.42 \text{ kJ/mol},$$

$$\Delta\bar{S}_{Cu} = 3.47 \pm 1.13 \text{ J/(K mol)}.$$

According to previous reports [1, 11, 12] and the data in Fig. 1b, the Cu_3AsSe_4 compound is connected by tie lines to As_2Se_3 and elemental selenium. Therefore, the partial molar functions of copper are thermodynamic characteristics of the following potential-forming reaction (all of the substances are in a crystalline state):

$$Cu + 0.167As_2Se_3 + 0.833Se = 0.333Cu_3AsSe_4. \quad (3)$$

The standard thermodynamic functions of formation of the Cu_3AsSe_4 compound and its standard entropy were calculated using (3) and the following relations ($Z = G$ or H):

$$\Delta_f Z^0(Cu_3AsSe_4) = 3\Delta\bar{Z}_{Cu} + 0.5\Delta_f Z^0(As_2Se_3),$$

$$S^0(Cu_3AsSe_4) = 3\Delta\bar{S}_{Cu} + 3S^0(Cu) + 2.5S^0(Se) + 0.5S^0(As_2Se_3),$$

We obtained

$$\Delta_f G^0(298 \text{ K}) = -147.3 \pm 0.5 \text{ kJ/mol},$$

$$\Delta_f H^0(298 \text{ K}) = -146.3 \pm 1.5 \text{ kJ/mol},$$

$$S^0(298 \text{ K}) = 307 \pm 13 \text{ J/(K mol)}.$$

Table 2. Univariant equilibria in the Cu_2Se–Cu_3AsSe_4–Se system

Curve in Fig. 5	Equilibrium	T, K
e_1M; $M'U_1$	$L \leftrightarrow \alpha + (Cu_3AsSe_4)_{1(II)}$	743–710; 710–645
p_1U_1	$L + \alpha \leftrightarrow (CuSe)_{III}$	650–645
p_2U_2	$L + (CuSe)_{III} \leftrightarrow CuSe_2$	605–600
U_1U_2	$L \leftrightarrow (CuSe)_{III} + (Cu_3AsSe_4)_I$	645–600
U_2E	$L \leftrightarrow CuSe_2 + (Cu_3AsSe_4)_I$	600–490
e_2E	$L \leftrightarrow CuSe_2 + Se$	494–490
e_3E	$L \leftrightarrow (Cu_3AsSe_4)_I + Se$	492–490
$m_1M(m_1'M')$	$L_1 \leftrightarrow L_2 + \alpha$	795–695
$m_2M(m_2'M')$	$L_1 \leftrightarrow L_2 + (Cu_3AsSe_4)_I$	713–695

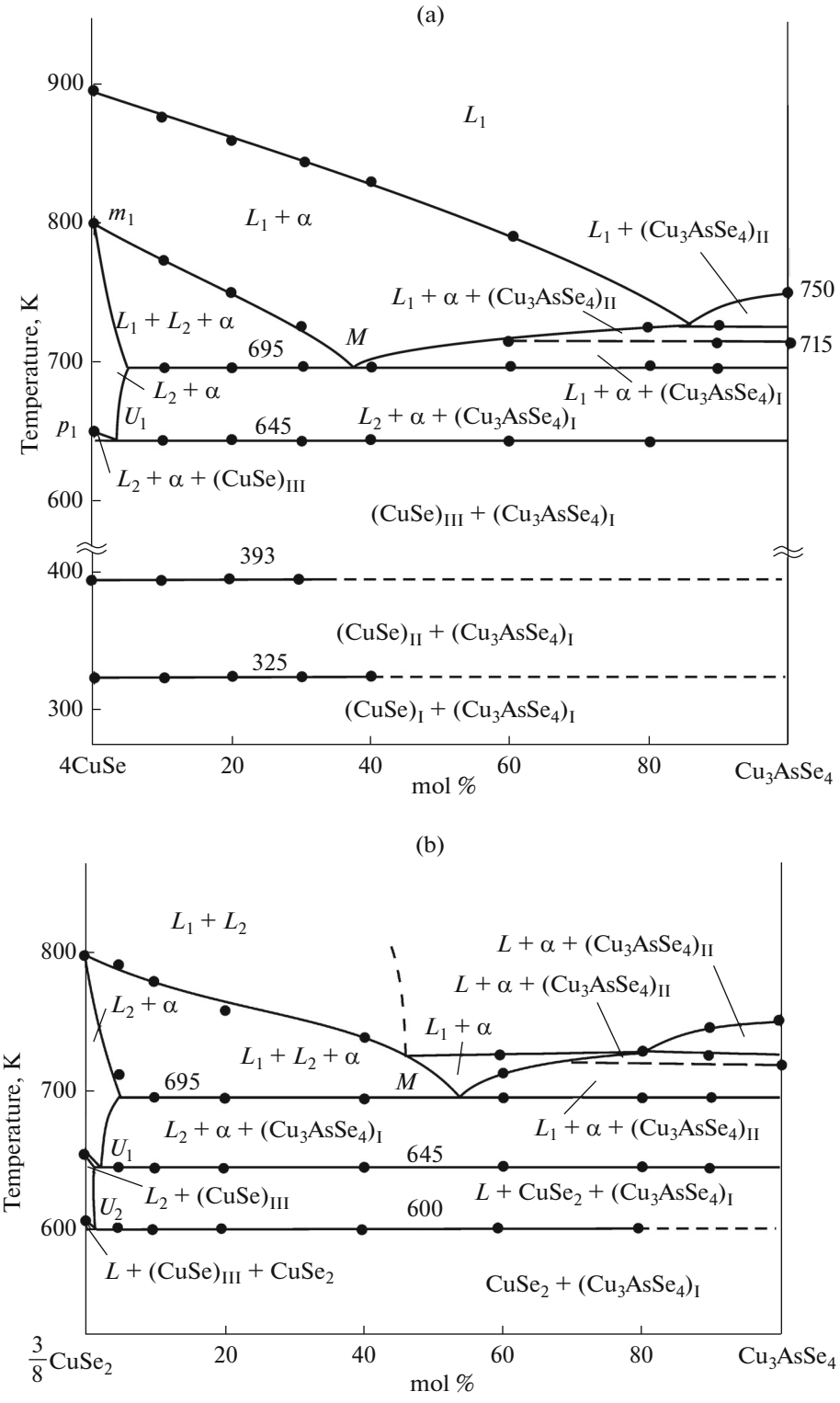

Fig. 4. (a) $CuSe–Cu_3AsSe_4$ and (b) $CuSe_2–Cu_3AsSe_4$ vertical sections through the phase diagram of the $Cu_2Se–Cu_3AsSe_4–Se$ system.

In our calculations, in addition to the present experimental data we used the previously reported standard entropies of copper (33.09 ± 0.08 J/(K mol)) and selenium (42.13 ± 2.09 J/(K mol)) [26, 27] and a mutually consistent data set obtained for As_2Se_3 by emf measurements [28]: ($\Delta_f G^0 = -55.26 \pm 0.58$ kJ/mol, $\Delta_f H^0 = -59.4 \pm 3.9$ kJ/mol, and $S^0 = 184.4 \pm 8.2$ J/(K mol). The previously reported data [28] agree well with cal-

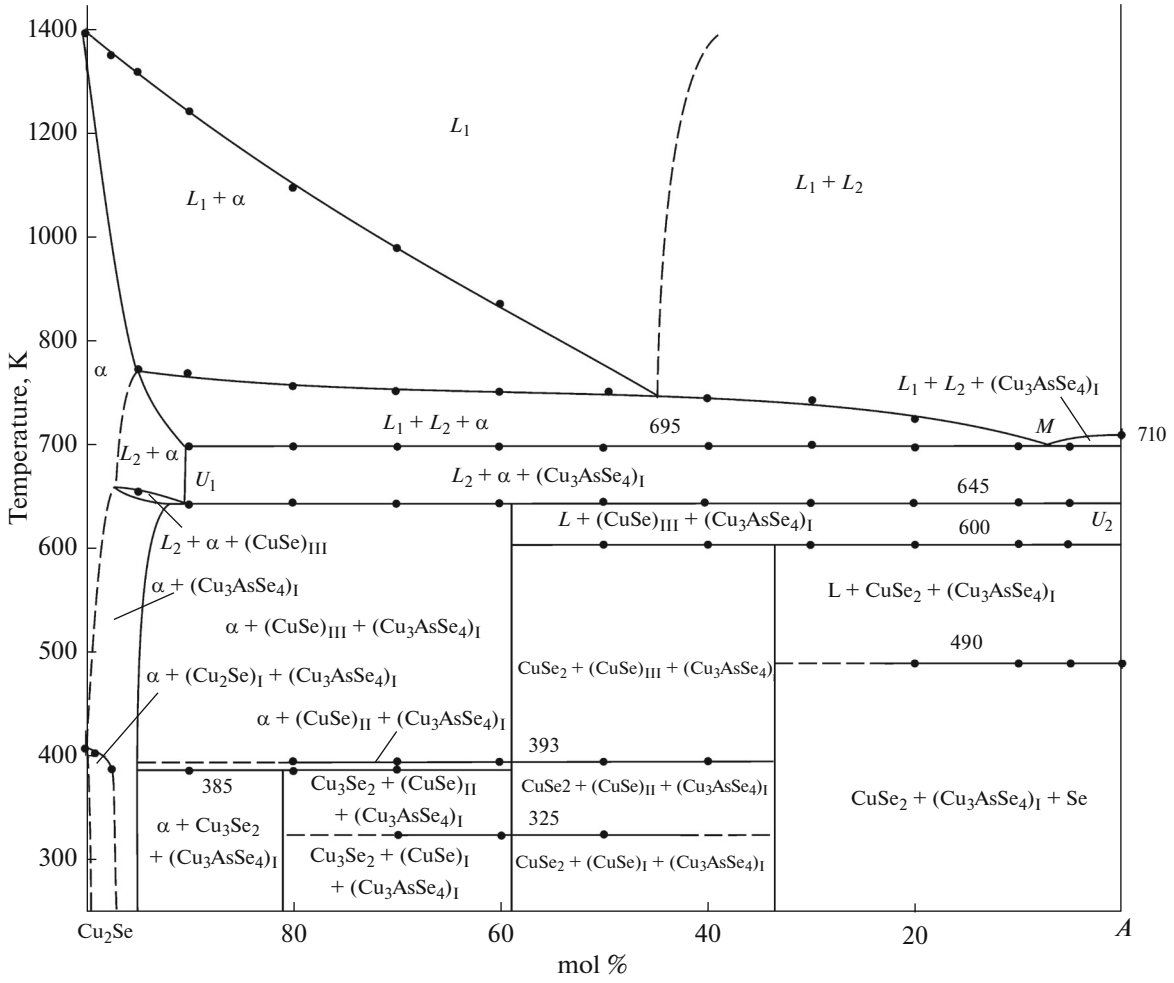

Fig. 5. $CuSe_2$–[*A*] vertical section through the phase diagram of the Cu_2Se–Cu_3AsSe_4–Se system.

orimetry results [29] ($\Delta_f H^0 = -56.7 \pm 6.0$ kJ/mol) and the standard entropy indicated in handbooks (194.6 ± 5.0 J/(K mol)).

CONCLUSIONS

The liquidus surface of the Cu_2Se–Cu_3AsSe_4–Se system comprises the primary crystallization fields of the high-temperature phases of Cu_2Se and Cu_3AsSe_4. The primary crystallization fields of the other copper selenides and selenium are degenerate. The system contains a broad liquid–liquid immiscibility region, which covers a significant part of the composition triangle. Using emf data, we have calculated the standard thermodynamic functions of formation and standard entropy of the low-temperature phase of Cu_3AsSe_4.

ACKNOWLEDGMENTS

This research was supported by the Science Foundation, State Oil Company of Azerbaijan Republic (Preparation and Characterization of Novel Functional Materials Based on Multicomponent Metal Chalcogenides for Alternative Energy Sources and Electronic Engineering Project, 2014).

REFERENCES

1. *Dvoinye i mnogokomponentnye sistemy na osnove medi: Spravochnik* (Binary and Multicomponent Copper Systems: A Handbook), Abrikosov, N.Kh., Ed., Moscow: Nauka, 1979.
2. Lazarev, V.B., Berul', S.I., and Salov, A.V., *Troinye poluprovodnikovye soedineniya v sistemakh A^I–B^V–C^{VI}* (Ternary Semiconductors in I–V–VI Systems), Moscow: Nauka, 1982.
3. Babanly, M.B., Yusibov, Yu.A., and Abishev, V.T., *Trekhkomponentnye khal'kogenidy na osnove medi i serebra* (Ternary Copper and Silver Chalcogenides), Baku: Bakinsk. Gos. Univ., 1993.
4. Avellaneda, D., Nair, M.T.S., and Nair, P.K., Cu_2SnS_3 and Cu_4SnS_4 thin films via chemical deposition for photovoltaic application, *J. Electrochem. Soc.,* 2010, vol. 157, no. 6, pp. D346–D352.

5. Marcano, G., Bracho, D.B., Rincon, C., Perez, G.S., and Nieves, L., On the temperature dependence of the electrical and optical properties of Cu_2GeSe_3, *J. Appl. Phys.,* 2000, vol. 88, pp. 822–828.

6. Morelli, D.T. and Skoug, E.J., Ternary copper-based diamond-like semiconductors for thermoelectric applications, *2009 MRS Spring Meet.: Materials and Devices for Thermal-to-Electric Energy Conversion,* San Francisco, 2009, vol. 1166, pp. 171–176.

7. Ivanov-Schitz, A.K. and Murin, I.V., *Ionika tverdogo tela (Solid State Ionics)*, St. Petersburg: S.-Peterburg. Univ., 2000, vol. 1.

8. Babanly, M.B., Yusibov, Y.A., and Babanly, N.B., *The EMF method with solid-state electrolyte in the thermodynamic investigation of ternary copper and silver chalcogenides, Electromotive Force and Measurement in Several Systems,* Kara, S., Ed., InTech, 2011, pp. 57–78.

9. Popesku, M.A., *Non-crystalline Chalcogenides,* Berlin: Springer, 2001.

10. Xin, S., Liu, J., and Salmon, P., Structure of Cu–As–Se glasses investigated by neutron diffraction with copper isotope substitution, *Phys. Rev. B: Condens. Matter Mater. Phys.,* 2008, vol. 78, no. 6, paper 064 207.

11. Tédenac, J.-C., *Arsenic–copper–selenium, Ternary Alloys,* Petzow, G., Ed., Weinheim: VCH, 1994, vol. 10, pp. 129–134.

12. Cohen, K., Rivet, J., and Dugue, J., Description of the Cu–As–Se ternary system, *J. Alloys Compd.,* 1995, vol. 224, pp. 316–329.

13. *Binary Alloy Phase Diagrams,* Massalski, T.B., Ed., Materials Park: ASM International, 1990, 2nd ed.

14. *Diagrammy sostoyaniya dvoinykh metallicheskikh sistem. Spravochnik* (Phase Diagrams of Binary Metallic Systems: A Handbook), Lyakishev, N.P., Ed., Moscow: Mashinostroenie, 1997, vol. 2.

15. Blachnik, R. and Gather, B., Enthalpies of melting of some ternary ABX_2-compounds (A = Cu, Ag; B = As, Sb, Bi; X = S, Se, Te), *Z. Naturforsch., B: Chem. Sci.,* 1972, vol. 27, no. 11, pp. 1417–420.

16. Potorii, M.V., Preparation and physicochemical properties of ternary selenides in I–V–VI systems, *Extended Abstract of Cand. Sci. (Chem.) Dissertation,* Lvov: Lvov State Univ., 1980.

17. Emsley, J., *The Elements,* Oxford: Clarendon, 1991

18. Glazov, V.M., Burkhanov, A.S., and Saleeva, N.M., A procedure for the preparation of single-phase copper and silver chalcogenides, *Izv. Akad. Nauk SSSR, Neorg. Mater.,* 1977, vol. 13, no. 5, pp. 917–919.

19. Morachevskii, A.G., Voronin, G.F., Geiderikh, V.A., and Kutsenok, I.B., *Elektrokhimicheskie metody issledovaniya v termodinamike metallicheskikh sistem* (Electrochemical Methods of Investigation in Thermodynamics of Metal Systems), Moscow: ITsK Akademkniga, 2003.

20. Babanly, M.B., Gasanova, Z.T., Mashadieva, L.F., Zlomanov, V.P., and Yusibov, Yu.A., Thermodynamic study of the Cu–As–S system by emf measurements with $Cu_4RbCl_3I_2$ as a solid electrolyte, *Inorg. Mater,* 2012, vol. 48, no. 3, pp. 225–228.

21. Babanly, N.B., Salimov, Z.E., Akhmedov, M.M., and Babanly, M.B., Thermodynamic study of Cu–Tl–Te system using emf technique with $Cu_4RbCl_3I_2$ solid electrolyte, *Russ. J. Electrochem.,* 2012, vol. 48, no. 1, pp. 68–73.

22. Babanly, M.B. and Yusibov, Yu.A., *Elektrokhimicheskie metody v termodinamike neorganicheskikh sistem* (Electrochemical Methods in Thermodynamics of Inorganic Systems), Baku: ELM, 2011.

23. Babanly, N.B., Yusibov, Yu.A., Aliev, Z.S., and Babanly, M.B., Phase equilibria in the Cu–Bi–Se system and thermodynamic properties of copper selenobismuthates, *Russ. J. Inorg. Chem.,* 2010, vol 55, no. 9, pp. 1471–1481.

24. Babanly, N.B., Aliev, Z.S., Yusibov, Yu.A., and Babanly, M.B., A Thermodynamic study of Cu–Tl–S system by emf method with $Cu_4RbCl_3I_2$ solid electrolyte, *Russ. J. Electrochem.,* 2010, vol. 46, no. 3, pp. 354–358.

25. Abbasov, A.S., Azizov, T.Kh., Aliev, I.Ya., and Mustafaev, F.M., Thermodynamic study of III–V, III-VI, and I–VI semiconductor systems, in *Termodinamicheskie svoistva metallicheskikh sistem* (Thermodynamic Properties of Metallic Systems), Baku: Elm, 1975, pp. 404–416.

26. *Baza dannykh "Termicheskie konstanty veshchestv". Elektronnaya versiya* (Thermal Constants of Substances Database, Electronic Version), Iorish, V.S. and Yungman, V.S., Eds., 2006. http://www/chem.msu.su/cgi-bin/tkv.

27. Kubaschewski, O., Alcock, C.B., and Spencer, P.J., *Materials Thermochemistry,* Oxford: Pergamon, 1993.

28. Babanly, D.M., Velieva, G.M., Imamaliyeva, S.Z., and Babanly, M.B., Thermodynamic functions of arsenic selenides, *Russ. J. Phys. Chem. A,* 2017, vol. 91, no. 7, pp. 1170–1173.

29. O'Hare, P.A.G., Calorimetric measurements of the specific energies of reaction of arsenic and of selenium with fluorine. Standard molar enthalpies of formation at the temperature 298.15 K of AsF_5, SeF_6, As_2Se_3, As_4S_4, and As_2S_3, *J. Chem. Thermodyn.,* 1993, vol. 25, no. 2, pp. 391–402.